

CrystEngComm

Accepted Manuscript



This is an *Accepted Manuscript*, which has been through the Royal Society of Chemistry peer review process and has been accepted for publication.

Accepted Manuscripts are published online shortly after acceptance, before technical editing, formatting and proof reading. Using this free service, authors can make their results available to the community, in citable form, before we publish the edited article. We will replace this *Accepted Manuscript* with the edited and formatted *Advance Article* as soon as it is available.

You can find more information about *Accepted Manuscripts* in the [Information for Authors](#).

Please note that technical editing may introduce minor changes to the text and/or graphics, which may alter content. The journal's standard [Terms & Conditions](#) and the [Ethical guidelines](#) still apply. In no event shall the Royal Society of Chemistry be held responsible for any errors or omissions in this *Accepted Manuscript* or any consequences arising from the use of any information it contains.

ARTICLE

Structural characterization of form I of anhydrous rifampicin

Cite this: DOI: 10.1039/x0xx00000x

Amanda Laura Ibiapino,^a Rafael Cardoso Seiceira,^b Altivo Pitaluga Jr.,^c Antonio Carlos Trindade^d and Fabio Furlan Ferreira^{a*}

Received 00th June 2014,
Accepted 00th June 2014

DOI: 10.1039/x0xx00000x

www.rsc.org/

Rifampicin is a first-line drug widely used in the treatment of tuberculosis both in the intensive as well as in the treatment phase. In this work we characterized the crystal structure of form I of anhydrous rifampicin, mainly by using X-ray powder diffraction data combined with the Rietveld method. Other complementary techniques such as Fourier transform infrared spectroscopy and thermal analysis were also employed. It crystallized in a monoclinic crystal system with space group *C*2 and unit cell parameters: *a* = 25.8846(2) Å, *b* = 14.2965(2) Å, *c* = 14.2796(2) Å, β = 122.98(1)°, *V* = 4432.81(7) Å³, *Z* = 4, *Z'* = 1 and ρ_{calc} = 1.23310(2) g cm⁻³. A BFDH model was used to inspect the crystal morphology prediction and great similarity with crystal observed on an optical microscope was found. The FTIR spectrum confirmed the results obtained by X-ray powder diffraction that all the functional groups involved in H-bonding are intramolecularly connected. This polymorphic form presented a thermal stability up to approximately 230 °C.

Introduction

Tuberculosis (TB) is an infectious disease caused by a pathogenic aerobic bacteria – *Mycobacterium tuberculosis*.¹⁻³ It is mainly transmitted through the air and can reach all organs of the body. However, as the bacteria reproduces and develops rapidly in areas of the body with high concentrations of oxygen, the lung becomes the main affected organ by the disease.⁴ The symptoms of TB usually are chronic cough, fever, night sweats, chest pain, anorexia and adynamia.⁴

Currently, the drugs used to treat tuberculosis can be divided into first- and second-line. Among the first-line drugs, isoniazid (INH), rifampicin (RMP), ethambutol (EMB), pyrazinamide (PZA), streptomycin (SM) and fluoroquinolones (ciprofloxacin and ofloxacin); and as second-line ones, cycloserine (Cs) para-amino-salicylic acid (PAS), ethionamide (Et), among others, can be found.⁴

RMP is considered the main component for the treatment of tuberculosis in conjunction with other first-line anti-TB drugs, being used both in the intensive phase as well as in the maintenance of treatment.⁵ Discovered in the 1960's, RMP is a semisynthetic antibiotic of the family of rifamycins – a rifamycin B-derivative – produced by strains of *Nocardia (Streptomyces) mediterranei*. It is officially designated by the IUPAC (International Union of Pure and Applied Chemistry) as (7S,11S,12R,13S,14R,15R,16R,17S,18S,19Z,21Z) 2,15,17,27,29-pentahydroxy-11-ethoxy-3,7,12,14,16,18,22-heptamethyl-26-[(E)-N-(4-

methylpiperazin-1-yl)carboximidoyl]-6,23-dioxo-8,30-dioxo-24-azatetracyclo[23.3.1.1^{4,7}.0^{5,28}]triacenta-1,3,5(28),9,19,21,25(29),26-octaen-13-yl acetate, with molecular formula C₄₃H₅₈N₄O₁₂ and molecular mass of 822.94 g mol⁻¹.^{6,7}

It is a complex molecule (Fig. 1), displaying different conformations due to the interactions between its functional groups, thus promoting different crystal morphologies.⁸ It is presented as a red-brown-colored crystalline powder.

Due to its complex structure, RMP exhibits polymorphism,^{9,10} existing in two polymorphic forms – form I and form II. Form I is considered stable while form II is metastable. Besides these two polymorphic forms, RMP is found as hydrates (monohydrate, dihydrate and pentahydrate),^{10,11} solvate,¹² and also in amorphous form.¹³ The existence of different solid states of RMP is constantly reported as one of the reasons for its low bioavailability, when RMP is alone in a medicine or combined with other anti-TB drugs, such as INH, PZA, and EMB.^{5,8,14-16}

It is worth noting although the phenomenon of polymorphism is known for more than two centuries, the pharmaceutical industry has began to study it with more emphasis only at the early 1960's, but many efforts to understand and assess the impact of polymorphism on pharmaceuticals have been performed only in recent decades.^{17,18} Currently, the study of polymorphism in the pharmaceutical industry has gained increased attention in the

pre-formulation stage, since two polymorphs of the same compound can display so different crystal structures as well as properties as two distinct compounds.¹⁹ Thus, differences in the physicochemical properties of polymorphs such as density, hardness, compressibility, refractive index, melting point, heat of fusion, vapor pressure, solubility and dissolution rate,²⁰ have important effects on the processing and stability of drugs in tablets, while differences in solubility and dissolution rate may have implications in their absorption, and consequently in the bioavailability.

Furthermore, the occurrence of polymorphic transition when the pharmaceuticals are already on the shelf can cause serious risks to the consumer. Hence, the characterization of drugs becomes one of the most important steps in the pharmaceutical industry, especially when one wants to bring to market a new formulation. In general, the most stable form exhibits higher melting point, lower solubility and maximum chemical stability. The metastable form, however, can exhibit chemical and physical stabilities sufficient in the conditions of shelf to justify their use.¹⁸

To shed some light on the study of polymorphism of rifampicin herein we show for the first time, as far as we are concerned, the crystal structure determination of form I of anhydrous RMP by means of a simulated annealing procedure using X-ray powder diffraction (XRPD) data. The final structure was then refined with the Rietveld method (RM). Complementary experimental techniques – Fourier transform infrared spectroscopy (FTIR), differential scanning calorimetry (DSC) and thermogravimetry (TG) – were also used.

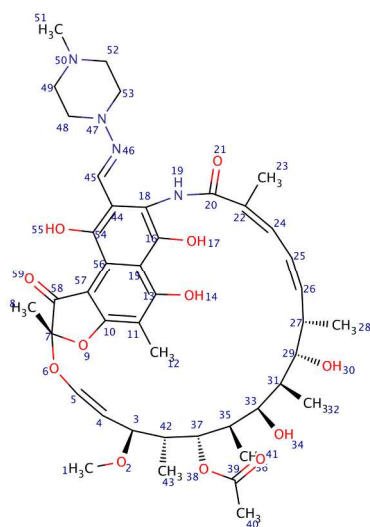


Fig. 1 Chemical structure of rifampicin. The numbering sequence was adopted following the IUPAC designation.

Experimental section

Material

A powdered sample of form I of anhydrous RMP (lot number will not be disclosed due to a confidential agreement) was kindly gifted by Farmanguinhos, Oswaldo Cruz Foundation (FIOCRUZ), RJ, Brazil.

X-ray powder diffraction

X-ray powder diffraction data of form I of anhydrous RMP were collected on a STADI-P diffractometer (Stoe®, Darmstadt, Germany), located at the Laboratory of Crystallography and Structural Characterization of Materials (LCCEM) of the Federal University of ABC (UFABC), operating in transmission geometry at 40 kV and 40 mA, using $\text{CuK}\alpha_1$ ($\lambda = 1.54056 \text{ \AA}$) radiation filtered by a primary beam monochromator (Ge (111) curved crystal), equipped with a 0.5-mm divergence slit and a 3-mm circular scattering slit and a silicon strip detector (Mythen 1K, from Dectris®, Baden, Switzerland). The measurement was performed in the angular range from 3° to 59.695° (2θ) with steps of 0.005° and integration time of 60 s at each 1.05° . The sample was loaded between two cellulose-acetate foils (Ultraplan®, 0.014-mm thick and density of 1.3 g cm^{-3} , which was spun during data collection.

Fourier transform infrared spectroscopy (FTIR)

The absorption spectrum in the infrared region was acquired using a Varian 660-IR spectrophotometer, equipped with an attenuated total reflectance (ATR) accessory using a ZnSe crystal at room temperature, with a resolution of 4 cm^{-1} in the range from 4000 to 650 cm^{-1} .

Thermogravimetry (TG)

The TG data were recorded using a *TGA Q-500* equipment from *TA Instruments* under a dynamic O_2 atmosphere (60 mL min^{-1}). Approximately 8 mg of sample were loaded in a Pt pan. The measurement was performed with a heating rate of $10 \text{ }^\circ\text{C min}^{-1}$, in the temperature range from 25 to $700 \text{ }^\circ\text{C}$.

Differential scanning calorimetry (DSC)

The DSC measurement was performed using a *DSC Q-200* from *TA Instruments*, under a dynamic N_2 atmosphere (50 mL min^{-1}) and a heating rate of $10 \text{ }^\circ\text{C min}^{-1}$, in the temperature range between 25 and $500 \text{ }^\circ\text{C}$. Approximately 6 mg of sample were hermetically sealed in an aluminum pan.

Results and discussion

Structure determination

After collecting the XRPD data of form I of anhydrous RMP, we conducted a search on the Cambridge Structural Database (CSD)²¹ to verify any possible similarity with the available data reported on the literature. Fig. 2 shows the experimental X-ray diffractogram of form I of anhydrous RMP together with the simulated diffractograms of different solvates of rifampicin, identified by their CSD REFCODEs: HAXWUA,¹² MAPHES,²² MAPHIW,²² OWELOS,²³ OWELUY²³ and RIFAMP.²⁴

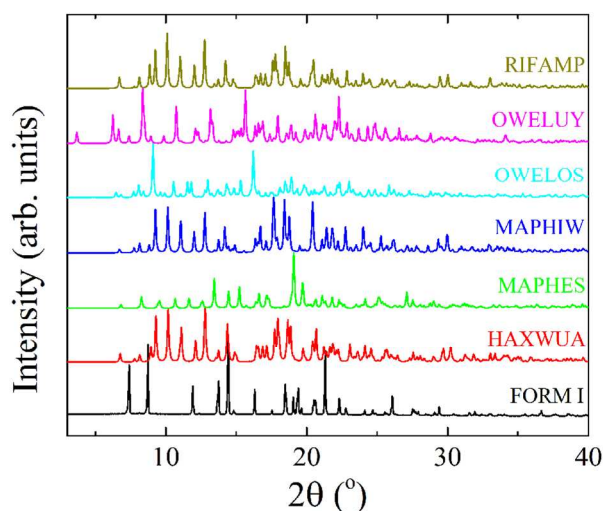


Fig. 2 Experimental X-ray diffractogram of form I of anhydrous RMP (black line) and calculated ones found in the CSD database with the following REFCODES: HAXWUA¹² (red line), MAPHES²² (green line), MAPHIW²² (blue line), OWELOS²³ (cyan line), OWELUY²³ (magenta line) and RIFAMP²⁴ (dark yellow line).

A close inspection on all diffractograms clearly indicates we are dealing with an unindexed data. So, we used the first 22 reflections of the X-ray diffractogram to index the pattern utilizing the software *Topas-Academic* v.5²⁵. The region delimited by those peaks was fitted without taking into account corrections for the zero point of the diffractometer and the Lorentz-Polarization factor. After analyzing the systematic absences it could be verified this polymorph crystallized in a monoclinic crystal system with space group *C2*, with unit cell parameters: $a = 25.8544 \text{ \AA}$, $b = 14.2798 \text{ \AA}$, $c = 14.2639 \text{ \AA}$, $\beta = 122.944^\circ$ and $V = 4419.40 \text{ \AA}^3$. A very satisfying Pawley²⁶ fit was obtained resulting in the following values for the unit cell parameters: $a = 25.8739(5) \text{ \AA}$, $b = 14.2922(3) \text{ \AA}$, $c = 14.2748(3) \text{ \AA}$, $\beta = 122.9778(4)^\circ$ and $V = 4428.3(2) \text{ \AA}^3$, which were then used as input for the structure determination procedure, carried out by means of a simulated annealing procedure implemented into the DASH program.²⁷ Detailed procedures may be found elsewhere.²⁸⁻³¹ A 3D model of the rifampicin molecule was created with the program *MarvinSketch* v. 6.2.1, which was then used in the simulated annealing procedure.^{32,33} The full range of possible values of molecular positions and orientations as well as any flexible torsion angles (three describing the positional coordinates, four, of which three are independent, describing the molecular orientation and six flexible torsion angles) were allowed to vary during the simulated annealing process. Fifteen runs (for a total of 2.25×10^8 movements) were globally optimized, and the best result was then considered in the final Rietveld refinement^{34,35} of the structure (shown in Fig. 3), using the program *Topas-Academic* v.5.³⁶ First of all, the unit cell parameters and the zero point of the diffractometer were refined. The background was fitted using a 20-term Chebyshev polynomial. The peak asymmetry was adjusted using the simple axial divergence model of Cheary and Coelho.^{37,38} The peak profiles were

modelled using the Double-Voigt approach³⁹ with the anisotropic peak profiles adjusted using 4-term spherical harmonics⁴⁰. The isotropic atomic displacements (B_{iso}) were constrained to be equal for all non-hydrogen atoms. For hydrogen atoms, the B_{iso} values were constrained to be 1.2 times larger than the values of the respective atoms to which they were connected. Their fractional coordinates were refined by using a macro implemented in *Topas-Academic* that “rides” (restrains the distances between hydrogen and neighboring atoms) the H atoms to the ones they are associated. At first, their fractional coordinates were inserted as the ones provided by Mercury. Then, taking into account the mean bond distance values found in Mercury (C–H = 0.96 Å, N–H = 0.87 Å and O–H = 0.99 Å), the refinement was performed, thus providing the final atomic coordinates of all atoms. It should be mentioned that some possible misorientation of the H atoms might occur since Mercury automatically calculates their placement. The molecular geometry (space group choice, unit cell parameters, bond lengths, angles and torsions) was verified with both the PLATON⁴¹ and MOGUL⁴² packages. Although the ADDSYM routine implemented in PLATON did not detect any obvious extra crystallographic symmetry, the choice for space group (*C2*) was indicated as a non-standard representation for *I2*. CCDC ID: 1005126 contains the supplementary crystallographic data for this paper. These data can be obtained free of charge from the Cambridge Crystallographic Data Centre (www.ccdc.cam.ac.uk/data_request/cif). The final unit cell parameters, goodness-of-fit indicator as well as *R* factors⁴³ were, respectively: $a = 25.8846(2) \text{ \AA}$, $b = 14.2965(2) \text{ \AA}$, $c = 14.2796(2) \text{ \AA}$, $\beta = 122.98(1)^\circ$, $V = 4432.81(7) \text{ \AA}^3$, $Z = 4$, $Z' = 1$, $\rho_{calc} = 1.23310(2) \text{ g cm}^{-3}$, $\chi^2 = 1.661$, $R_{exp} = 2.341 \%$, $R_{wp} = 3.891 \%$ and $R_{Bragg} = 1.356 \%$. The crystal data and structure refinement details are displayed in Table 1.

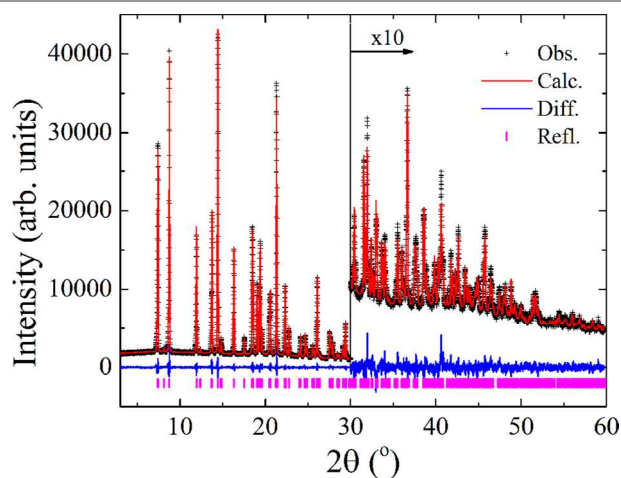


Fig. 3 Rietveld plot of form I of anhydrous RMP. Black crosses represent the observed pattern, while the red line indicate the calculated one. The blue line at the bottom displays the difference between the observed and calculated diffractograms. Magenta bars show the Bragg peaks. After 30° (2θ) the pattern was magnified (10x) for better visualization.

Table 1 Crystal data and details of the structure refinement for the form I of anhydrous rifampicin.

Crystal Data – Form I of anhydrous rifampicin	
Formula	C ₄₃ H ₅₈ N ₄ O ₁₂
Formula Weight (g mol ⁻¹)	822.93
Crystal System	Monoclinic
Space group	C2 (No. 5)
<i>a</i> , <i>b</i> , <i>c</i> (Å)	25.8844(2), 14.2964(2), 14.2795(2)
β (°)	122.98(1)
Volume (Å ³)	4432.7(5)
<i>Z</i> , <i>Z'</i>	4, 1
ρ _{calc} (g cm ⁻³)	1.23310(2)
<i>Data collection</i>	
Diffractometer	STADI-P, Stoe
Monochromator	Ge(111)
Wavelength (Å)	1.54056
2θ range (°)	3 – 59.695
Step size (°)	0.005
Time per 3.15° at 2θ (s)	60
Diffraction temperature (K)	298
<i>Refinement</i>	
Number of observations	11340
Number of contributing reflections	697
Number of distance constraints	155
<i>Number of refined parameters</i>	
Structural parameters	202
Profile parameters	7
<i>Statistical parameters</i>	
<i>R</i> _{exp} (%)	2.341
<i>R</i> _{wp} (%)	3.890
<i>R</i> _{Bragg} (%)	1.356
<i>S</i>	1.661
<i>d</i> - <i>DW</i> ^[a]	0.653

^[a]The weighted Durbin–Watson statistics (*d*-*DW*) is quite low,⁴⁴ indicating that the standard deviations are underestimated. There is no adequate physical model to correct the standard deviation values in the Rietveld method, to make them representative of the repetition of the experiment.

Structure description

The unit cell of form I of anhydrous RMP consists of four formula units per unit cell (*Z* = 4), accommodating one molecule in the asymmetric unit (*Z'* = 1). As expected,^{7,11} all the functional groups that can be involved in H-bonding are intramolecularly connected. The predicted intermolecular hydrogen bond propensities, calculated with the Mercury software, evidenced the same result.

An inspection of possible voids in the structure was performed with the Mercury software taking into account a probe radius of 1.4 Å, which corresponds to the size of a water molecule, and no available space for their insertion were found. Comparisons between the volumes of the solvates that present the same number of formula units per unit cell as the one reported herein (*Z* = 4) were made and also confirmed we are dealing with a more compact unit cell (RIFAMP → *V* = 4836.4 Å³, OWELUY → *V* = 5780.4 Å³, OWELOS → *V* = 10351.5 Å³, HAXWUA → *V* = 4755.5 Å³ and anhydrous form I → *V* = 4432.8 Å³). Also,

Analyses on least squares plane calculation on the 13-membered ring composed by atoms O(9)–C(7)–C(10)–C(11)–C(13)–C(15)–C(16)–C(18)–C(44)–C(54)–C(56)–C(57)–C(58) revealed that the atom C(7) is the most deviating one from

perfect planar ring, with the highest deviation from the least squares plane passing through this ring being 0.15(5) Å. The root mean square errors (rmse) of contributing atoms of the 13-membered ring displayed in Fig. 1 is equal to 0.06 Å, indicating a slight deviation from an almost planar system.

Fig. 4 shows the crystal structure of form I of anhydrous RMP with some intramolecular H-bonds represented by cyan lines. The intermolecular bonding occurs through the red lines represented in Fig. 4, with the terminal atom belonging to the neighboring molecule.

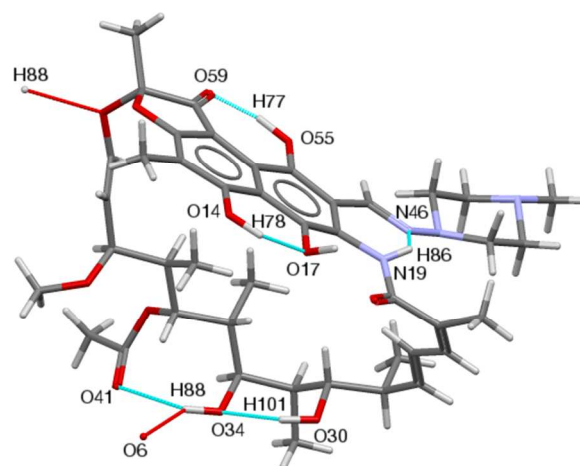


Fig. 4 Representation of the molecule of form I of anhydrous RMP contained in its unit cell. Intra and intermolecular H-bonds are indicated by lines (cyan and red, respectively).

Analysis on crystal morphology prediction, shown in Fig. 5, using the BFDH algorithm⁴⁵⁻⁴⁷ available in Mercury revealed great similarity with the crystals observed on an optical microscope (Olympus BX 51M equipped with a CCD Olympus Altra 20). The BFDH model takes into account some crystallographic geometrical considerations and assumes that the growth rate of the crystal face is inversely proportional to the interplanar spacing *d*_{*hkl*}. With this, the most morphologically relevant faces of the crystal are those having the largest *d*_{*hkl*} values:^{45,46} *d*₂₀₁ = 11.98 Å, *d*₁₁₀ = 11.94 Å, *d*₀₀₁ = 11.88 Å, *d*₂₀₀ = 10.86 Å and *d*₁₋₁₋₁ = 10.10 Å, as obtained during the indexing procedure. Due to the small variations on *d*, thus conferring an almost spherical character of the particles would imply in a greater stability of the crystals as well as in a lower solubility. Comparing the morphology prediction with the micrograph of the crystals, a good visual agreement is found.

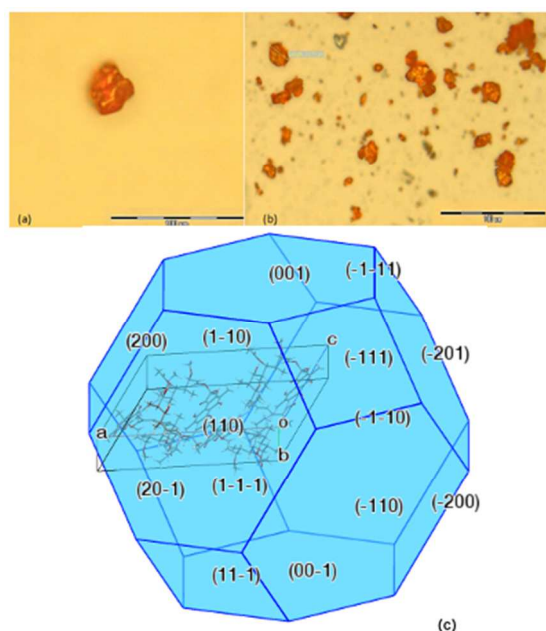


Fig. 5 Optical microscopy images of (a) an isolated crystal and (b) of several ones of form I of RMP; (c) crystal morphology prediction displaying some Miller indices on different faces of the crystal.

Fourier transform infrared spectroscopy (FTIR)

Fig. 6 displays the FTIR spectrum of form I of anhydrous RMP, obtained with a resolution of 4 cm^{-1} in the region $4000\text{--}650\text{ cm}^{-1}$, where the main absorption bands characterizing this drug are found.

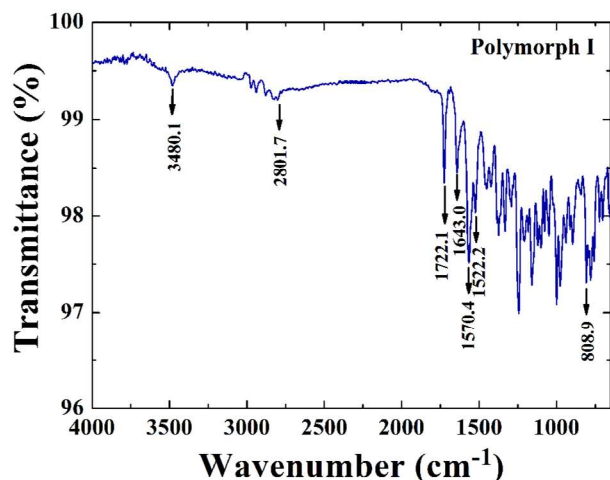


Fig. 6 FTIR spectrum of form I of anhydrous RMP, obtained with resolution of 4 cm^{-1} in the region $4000\text{--}650\text{ cm}^{-1}$.

The different crystal packing of rifampicin, attributed to the various possibilities of hydrogen bonding, conformational exchanges, and ionization states, is the clearest evidence of its polymorphism.⁹ All the functional groups that can be involved in H-bonding are intramolecularly bonded, also confirmed by our X-ray analysis, showing differences in OH of chain loop, acetyl group, furanone group and amide C=O frequencies.⁷ Such differences are important to distinguish polymorphic

forms of rifampicin. In order to better illustrate the possible different conformational arrangements of the structures, in Fig. 7 we can see the crystal packing of the anhydrous RMP form I with the solvates found in the CSD (RIFAMP,²⁴ MAPHES²² and HAXWUA¹²) that accommodate one formula unit per unit cell.

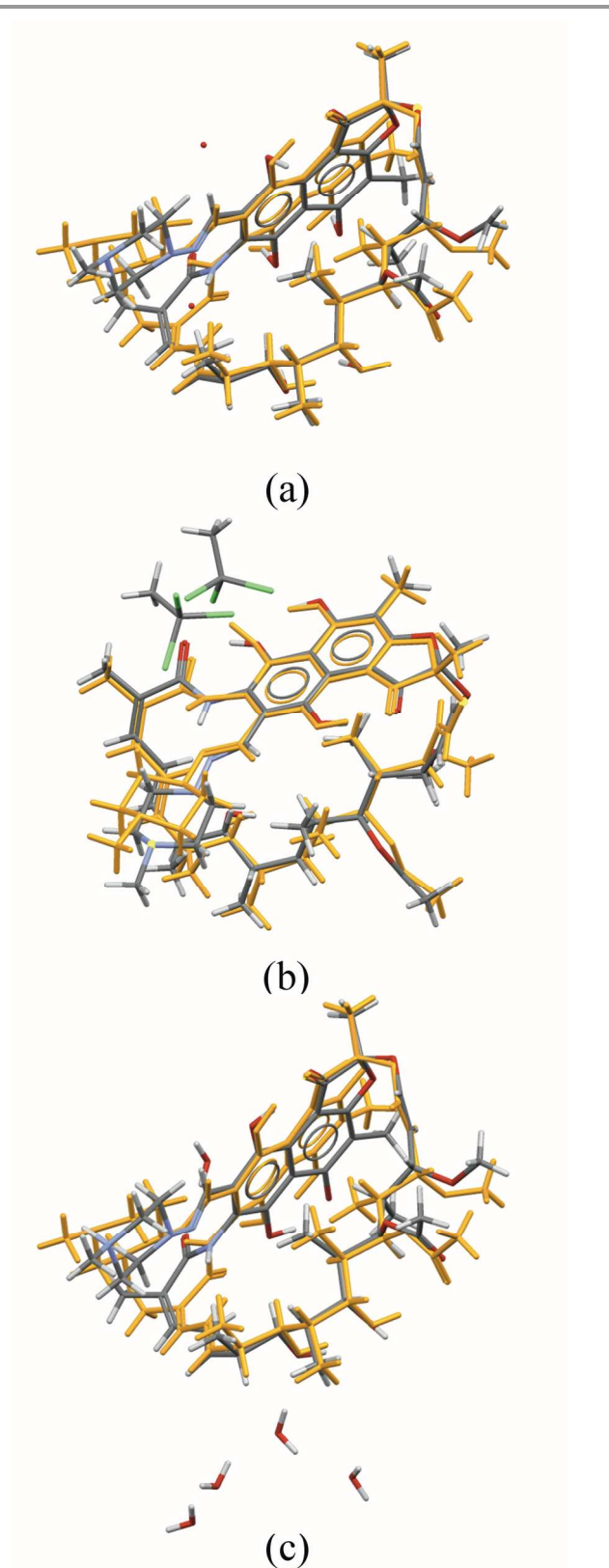


Fig. 7 Crystal packing overlays of the anhydrous RMP form I (orange molecule) with the different solvates found in the CSD that accommodate one formula unit per unit cell: (a) RIFAMP,²⁴ (b) MAPHES²² and (c) HAXWUA.¹²

From Fig. 6 it can be seen the absorption bands that characterize the form I of anhydrous RMP are found at about 3480 cm^{-1} (ansa OH), 2802 cm^{-1} (stretching N-CH₃),¹¹ 1722 cm^{-1} (acetyl C=O), 1643 cm^{-1} (furanone C=O),⁷ 1570 cm^{-1} (amide C=O),⁷ 1522 cm^{-1} (stretching N-C) and 809 cm^{-1} (rocking H-N and H-O).⁴⁸ A clear evidence we are dealing with an anhydrous sample is the absence in the FTIR spectrum of one overlapped band, attributed to water, at approximately $3600\text{--}2850\text{ cm}^{-1}$, which can be evidenced in samples of rifampicin called SI and SII (solvate with 5H₂O), as described in the literature.¹¹

Thermogravimetry (TG) and Differential Scanning Calorimetry (DSC)

The thermal behavior of form I of anhydrous RMP was evaluated by means of thermal analysis (TG and DSC). Fig. 8 and Fig. 9 present the TG/DTG and DSC curves of form I of anhydrous RMP, respectively. On the basis of the TG/DTG curves (Fig. 8) it was possible to verify this polymorphic form is thermally stable up to approximately $230\text{ }^{\circ}\text{C}$, close to values reported on the literature.⁶ Above this temperature, three events related to the thermal decomposition of the sample are observed. The first one, at $250\text{ }^{\circ}\text{C}$ (DTG), represents a mass loss of 23.3% (Δm); the second one, at $287\text{ }^{\circ}\text{C}$, corresponds to $\Delta m = 13.5\%$, and the third one, at $488\text{ }^{\circ}\text{C}$, refers to $\Delta m = 62.8\%$, the sample being completely degraded. Above this temperature is also observed a residue content of 0.1%.

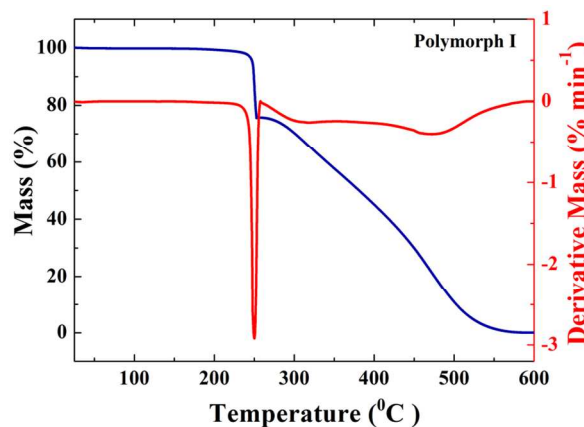


Fig. 8 TG (blue line)/DTG (red line) curves of the form I of anhydrous RMP obtained at $10\text{ }^{\circ}\text{C min}^{-1}$, under a dynamic atmosphere of O₂ (60 mL min^{-1}), with a sample weight of approximately 8 mg.

In the DSC curve displayed in Fig. 9 are evidenced two exothermic events – the first one at $266\text{ }^{\circ}\text{C}$ (T_{peak}),^{6,8,49} and the second at $357\text{ }^{\circ}\text{C}$ (T_{peak}) – both referring to the process of thermal decomposition of form I of rifampicin.⁶ We can infer we are dealing with an anhydrous form of rifampicin since it is not evidenced in the DSC curve one endothermic peak below $115\text{ }^{\circ}\text{C}$, which would indicate the presence of water in the sample of form I, and in TG/DTG curve no weight loss is found below $200\text{ }^{\circ}\text{C}$. According to Pelizza *et al.*, the release of adsorbed water as well as water of crystallization, which would

be inferred by endothermic peaks in the region between 140 and 160 °C, were evidenced in a pentahydrate solvate of rifampicin (named SI in ref. 11).¹¹ Also, when studying another pentahydrate sample (named SII in ref. 11) of rifampicin they observed endothermic peaks at about 98 °C and 115 °C, referring to the loss of water.¹¹ None of these are displayed in Fig. 9, thus supporting the character of an anhydrous form.

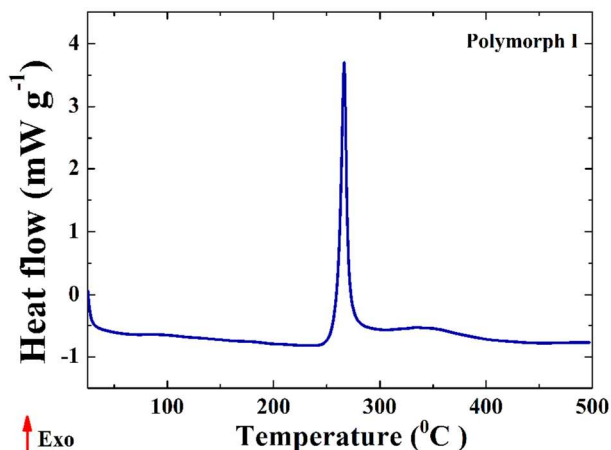


Fig. 9 DSC curve of form I of anhydrous RMP obtained at 10 °C min⁻¹, under a dynamic atmosphere of N₂ (50 mL min⁻¹), with a sample weight of about 6 mg.

It should be noted that the exothermic thermal events observed in the DSC curve (Fig. 9) are consistent with the events of mass loss shown in the TG/DTG curves of form I of anhydrous RMP (Fig. 8).

Conclusions

By means of XRPD, FTIR, TG and DSC we accurately characterized the crystal structure of form I of anhydrous RMP. It crystallized in a monoclinic crystal system with space group C2. The indices expressing the goodness of fit as well as R factors were: $\chi^2 = 1.661$, $R_{exp} = 2.341\%$, $R_{wp} = 3.891\%$ and $R_{Bragg} = 1.356\%$, and suggested a good procedure in the refinement.

By means of FTIR spectrum of form I of anhydrous RMP was shown that the absorption bands at approximately 3480 cm⁻¹, 2801 cm⁻¹, 1722 cm⁻¹, 1643 cm⁻¹, 1570 cm⁻¹, 1522 cm⁻¹ and 808 cm⁻¹ for the OH of chain loop group, stretching N-CH₃, acetyl group, furanone group, amide group, stretching N-C and rocking H-N and H-O respectively, were sufficient to characterize the form I of anhydrous RMP.

Thermal analysis and FTIR measurements gave evidence about the anhydrous character of RMP, since we could not observe endotherm peaks below 115 °C in the DSC curve and weight losses below 200 °C in TG/DTG curves. Also, some characteristic absorption bands, located between 3600-2850 cm⁻¹, which would indicate the presence of water, were not observed.

The characterization of drugs by different techniques has become of great importance for the pharmaceutical industry, especially in the stage of pre-formulation. And since it is

possible to occur polymorphic transformations that may impact the performance and quality of medicines, polymorphism investigations are important steps during the production chain.

Acknowledgements

We thank the financial support provided by the São Paulo State Foundation (Proc. FAPESP nr. 2008/10537-3), the National Council for Scientific and Technological Development (Proc. CNPq nr. 305186/2012-4 and 477296/2011-4), the Coordination for Improvement of Higher Education Personnel (CAPES) and UFABC.

Notes

^a Center of Natural and Human Sciences (CCNH), Federal University of ABC (UFABC), Av. dos Estados, 5001, Santo André, SP, 09210-580, Brazil.

*e-mail: fabio.furlan@ufabc.edu.br

^b Laboratory of Solid State Studies (LEES), Farmanguinhos, FIOCRUZ, Av. Comandante Guarany, 447, Rio de Janeiro, RJ, 22775-903, Brazil.

^c Real Time Process and Chemical Analysis Development Center (NQTR), Chemistry Institute, Federal University of Rio de Janeiro (UFRJ), Rua Hélio de Almeida, 40, Rio de Janeiro, RJ, 21941-614, Brazil.

^d Federal Institute of São Paulo (IFSP), Av. Mogi das Cruzes, 1501, Suzano, SP, 08673-010, Brazil.

† Electronic Supplementary Information (ESI) available: [X-ray crystallographic data in CIF format, tables for final atomic structural parameters as well as some selected bond lengths and bond angles.]. See DOI: 10.1039/b000000x/

References

- R. G. Ducati, A. Ruffino-Netto, L. A. Basso and D. S. Santos, *Mem. Inst. Oswaldo Cruz*, 2006, 101, 697-714.
- V. Shukla and F. V. Manvi, *Int. J. Drug Del.*, 2010, 2, 322-332.
- J. S. Blanchard, *Ann. Rev. Biochem.*, 1996, 65, 215-239.
- M. V. N. Souza and T. R. A. Vasconcelos, *Quim. Nova*, 2005, 28, 678-682.
- S. Agrawal and R. Panchagnula, *Int. J. Pharm.*, 2004, 287, 97-112.
- R. Alves, T. V. S. Reis, L. C. C. Silva, S. Storpirtis, L. P. Mercuri and J. R. Matos, *Braz. J. Pharm. Sci.*, 2010, 46, 343-351.
- S. Agrawal, Y. Ashokraj, P. V. Bharatam, O. Pillai and R. Panchagnula, *Eur. J. Pharm. Sci.*, 2004, 22, 127-144.
- M. Sosa, M. E. Széliga, A. Fernández and C. Bregni, *Ars Pharm.*, 2005, 46, 353-364.
- S. Q. Henwood, M. M. de Villiers, W. Liebenberg and A. P. Lotter, *Drug Dev. Ind. Pharm.*, 2000, 26, 403-408.
- C. Becker, J. B. Dressman, H. E. Junginger, S. Kopp, K. K. Midha, V. P. Shah and S. Stavchansky, *J. Pharm. Sci.*, 2009, 98, 2252-2267.
- G. Pelizza, M. Nebuloni, P. Ferrari and G. G. Gallo, *Il Farmaco*, 1977, 32, 471-481.
- B. Wicher, K. Pyta, P. Przybylski, E. Tykarska and M. Gdaniec, *Acta Crystallogr. C*, 2012, 68, 209-212.
- S. Q. Henwood, W. Liebenberg, L. R. Tiedt, A. P. Lotter and M. M. de Villiers, *Drug Dev. Ind. Pharm.*, 2001, 27, 1017-1030.
- S. Singh, T. T. Mariappan, R. Shankar, N. Sarda and B. Singh, *Int. J. Pharm.*, 2001, 228, 5-17.
- S. Singh, H. Bhutani and T. T. Mariappan, *Indian J. Tuberc.*, 2006, 53, 201-205.
- C. J. Shishoo, S. A. Shah, I. S. Rathod, S. S. Savale, J. S. Kotecha and P. B. Shah, *Int. J. Pharm.*, 1999, 190, 109-123.
- D. J. W. Grant and S. R. Byrn, *Adv. Drug Del. Rev.*, 2004, 56, 237-239.
- G. L. B. Araújo, A. Pitaluga Jr, S. G. Antonio, C. O. Paiva-Santos and J. R. Matos, *Rev. Ciênc. Farm. Básica Apl.*, 2012, 33.
- S. Storpirtis, R. Marcolongo, F. S. Gasparotto and C. M. Vilanova, *Ger. Medic. Infarma*, 2004, 16, 51-56.
- E. G. Sánchez, H. C. Jung, L. M. Yépez and V. Hernandez-Abad, *Rev. Mex. Cienc. Farm.*, 2007, 38, 57-76.

21. I. J. Bruno, J. C. Cole, P. R. Edgington, M. Kessler, C. F. Macrae, P. McCabe, J. Pearson and R. Taylor, *Acta Crystallogr. B*, 2002, 58, 389-397.
22. K. Pyta, P. Przybylski, B. Wicher, M. Gdaniec and J. Stefanska, *Org. Biomol. Chem.*, 2012, 10, 2385-2388.
23. M. M. de Villiers, M. R. Caira, J. Li, S. J. Strydom, S. A. Bourne and W. Liebenberg, *Mol. Pharm.*, 2011, 8, 877-888.
24. M. Gadret, M. Goursolle, J. M. Leger and J. C. Colleter, *Acta Crystallogr. B*, 1975, 31, 1454-1462.
25. A. A. Coelho, J. Evans, I. Evans, A. Kern and S. Parsons, *Powder Diffr.*, 2011, 26, s22-s25.
26. G. S. Pawley, *J Appl. Crystallogr.*, 1981, 14, 357-361.
27. W. I. F. David, K. Shankland, J. van de Streek, E. Pidcock, W. D. S. Motherwell and J. C. Cole, *J. Appl. Crystallogr.*, 2006, 39, 910-915.
28. F. F. Ferreira, S. G. Antonio, P. C. P. Rosa and C. O. Paiva-Santos, *J. Pharm. Sci.*, 2010, 99, 1734-1744.
29. F. F. Ferreira, A. C. Trindade, S. G. Antonio and C. de Oliveira Paiva-Santos, *CrystEngComm*, 2011, 13, 5474.
30. A. Gomez, S. G. Antonio, G. L. B. de Araujo, F. F. Ferreira and C. O. Paiva-Santos, *CrystEngComm*, 2012, 14, 2826-2830.
31. F. N. Costa, F. F. Ferreira, T. F. da Silva, E. J. Barreiro, L. M. Lima, D. Braz and R. C. Barroso, *Powder Diffr.*, 2013, 28, S491-S509.
32. E. Aarts and J. Korst, *Simulated Annealing and Boltzmann Machines: a Stochastic Approach to Combinatorial Optimization and Neural Computing*, E. Aarts and J. Korst, John Wiley & Sons, Chichester, UK, 2nd edn., 1991.
33. P. J. M. van Laarhoven and E. H. L. Aarts, *Simulated Annealing: Theory and Applications*, P. J. M. van Laarhoven and E. H. L. Aarts, Kluwer Academic Publishers, Dordrecht, Holland, 4th edn., 1992.
34. H. M. Rietveld, *Acta Crystallogr.*, 1967, 22, 151-152.
35. H. M. Rietveld, *J. Appl. Crystallogr.*, 1969, 2, 65-71.
36. A. A. Coelho, J. Evans, I. Evans, A. Kern and S. Parsons, *Powder Diffr.*, 2011, 26, S22-S25.
37. R. W. Cheary and A. A. Coelho, *J. Appl. Crystallogr.*, 1998, 31, 862-868.
38. R. W. Cheary and A. A. Coelho, *J. Appl. Crystallogr.*, 1998, 31, 851-861.
39. D. Balzar, *J. Res. Natl. Inst. Stand. Technol.*, 1993, 98, 321-353.
40. M. Jarvinen, *J. Appl. Crystallogr.*, 1993, 26, 525-531.
41. A. L. Spek, *J. Appl. Crystallogr.*, 2003, 36, 7-13.
42. I. J. Bruno, J. C. Cole, M. Kessler, J. Luo, W. D. S. Motherwell, L. H. Purkis, B. R. Smith, R. Taylor, R. I. Cooper, S. E. Harris and A. G. Orpen, *J. Chem. Inf. Comput. Sci.*, 2004, 44, 2133-2144.
43. B. H. Toby, *Powder Diffr.*, 2006, 21, 67-70.
44. R. J. Hill and H. D. Flack, *J. Appl. Crystallogr.*, 1987, 20, 356-361.
45. M. A. Bravais, *Études Cristallographiques*, Gauthier Villars, Paris, France, 1866.
46. G. Friedel, *Bull. Soc. Franc. Mineral.*, 1907, 30, 326-455.
47. J. D. H. Donnay and D. Harker, *Am. Mineral.*, 1937, 22, 446-467.
48. A. Favila, M. Gallo and D. Glossman-Mitnik, *J. Mol. Model.*, 2007, 13, 505-518.
49. F. D. Freire, C. F. S. Aragão, T. F. A. Lima e Moura and F. N. Raffin, *J. Thermal Anal. Calor.*, 2009, 97, 333-336.